Earthquake Engineering & Structural Dynamics
The Journal of the International Association for Earthquake Engineering

EARTHQUAKE ENGINEERING & STRUCTURAL DYNAMICS
Earthquake Engng Struct. Dyn. 2012; **41**:2351–2357
Published online 7 February 2012 in Wiley Online Library (wileyonlinelibrary.com). DOI: 10.1002/eqe.2167

SHORT COMMUNICATION

Inelastic displacement ratio of near-source pulse-like ground motions

Iunio Iervolino*,†, Eugenio Chioccarelli and Georgios Baltzopoulos

Dipartimento di Ingegneria Strutturale, Università degli Studi di Napoli Federico II, Naples, Italy

SUMMARY

Near-source pulse-like records resulting from rupture's directivity have been found to depart from so-called ordinary ground motions in terms of both elastic and inelastic structural seismic demands. In fact, response spectra may be strong if compared with what is expected from common ground motion prediction equations. Moreover, because not all spectral ordinates are affected uniformly, a peculiar spectral shape, with an especially amplified region depending on the pulse period, may follow. Consequently, inelastic seismic demand may show trends different to records not identified as pulse-like (i.e., ordinary). This latter aspect is addressed in the study reported in this short communication, where a relatively large dataset of identified impulsive near-source records is used to derive an analytical-form relationship for the inelastic displacement ratio. It is found that, similar to what was proposed in literature for soft soil sites, a double-opposite-bumps form is required to match the empirical data as a function of the structural period over the pulse period ratio. The relationship builds consistently on previous studies on the topic, yet displays different shape with respect to the most common equations for static structural assessment procedures.

Received 7 November 2011; Revised 29 December 2011; Accepted 2 January 2012

KEY WORDS: forward directivity; near-fault; coefficient method

1. INTRODUCTION

In near-source (NS) conditions, ground motions may show special characteristics that systematically affect seismic structural demand. This is believed to be due to rupture's forward directivity, which may show up at sites in particular geometrical configurations with respect to the rupture, and results in velocity fault-normal signals characterized by a large full-cycle pulse at the beginning of the record and containing most of its energy [1]. Previous studies (e.g., [2]), found effects on both elastic and inelastic seismic demand characterizing pulse-like records, if compared with those non-pulse-like (hereafter *ordinary*).

The features of NS pulse-like records that may be of structural interest are: (1) ground motion is characterized by fault normal (FN) rotated record of generally larger amplitude than the fault parallel (FP), while non-pulse-like ground motions have *equivalent* FN and FP components; (2) FN pulse-like signals are characterized by a nonstandard pseudoacceleration spectral shape with an increment of spectral ordinates in a range around the pulse period (T_p), that is, a *bump* shape; (3) inelastic to elastic seismic spectral displacement ratio for FN pulse-like records may virtually depart from the *equal displacement rule*, and can be higher than that of ordinary motions. Increments are displayed in a range of period between about 30% and 50% of pulse period.

*Correspondence to: Iunio Iervolino, Dipartimento di Ingegneria Strutturale, Università degli Studi di Napoli Federico II, via Claudio 21, 80125, Naples, Italy.
†E-mail: iunio.iervolino@unina.it

Issues (1) and (2) refer to elastic seismic demand, and call for investigations about the need and feasibility to account for them in probabilistic seismic hazard analysis. Such studies are currently in progress (e.g., [3–5]). Issue (3) refers to inelastic demand, and is the subject of this communication, in which the inelastic to elastic displacement ratio, or C_R, is studied by means of semi-empirical relationships (e.g., [6]). In Equation (1), $S_{d,e}(T)$ is the elastic spectral displacement at period T and $S_{d,i}(T)$ is its inelastic counterpart for a given strength reduction factor (usually indicated as R or R_s).

$$C_R = S_{d,i}(T)/S_{d,e}(T) \tag{1}$$

Current static structural assessment procedures (e.g., [7]) rely on prediction equations for this kind of parameters to estimate inelastic seismic demand given the (elastic) seismic hazard. Because such relationships have to be estimated semi-empirically, in those cases where peculiar features in ground motions are expected, it is necessary to investigate whether they may show special trends (e.g., [8]). In fact, inelastic displacement for near-source conditions was studied already by a number of researchers (e.g., [9, 10]). The most up to date study with respect to this issue and dealing with pulse-like records is that in [11], which also motivates this study pointing out the need for further investigation on the C_R functional form. This is the scope of the study herein presented, where a series of bilinear (with 3% post-elastic stiffness) SDOF systems were analyzed when subjected to: (i) sets of FN impulsive records; (ii) the corresponding FP components; and (iii) a set of ordinary ground motions. The SDOF systems were designed to cover different nonlinearity levels, measured by means of R. The latter is given in Equation (2), where: $S_{a,e}(T)$ is the elastic spectral acceleration, m is the mass of the SDOF system, and F_y is the yielding strength in the case of bilinear hysteresis' backbone (yielding strength was changed record by record to have uniform strength reduction factor, that is, a constant R approach). Results were employed to fit the observed trends, which were found to be different if compared with those of ordinary and FP records (at least in terms of amplitude in this latter case), as a function of the T over T_p ratio.

$$R = S_{a,e}(T)\cdot m/F_y \qquad R = \{2, 3, \ldots, 8\} \tag{2}$$

In the following, dataset and empirical trends are briefly described first, then the discussion of chosen functional form is given, along with a description of the regression strategy. Finally, results are presented and discussed with respect to background research.

2. DATASET AND EMPIRICAL EVIDENCE

The pulse-like records considered are a set, from Ref. [2], identified with the algorithm in [12], which is extremely useful because it allows to remove most of the subjectivity in the analysis of directivity in ground motion (which comes in the usual approach of visual inspection of waveforms) and to search large datasets, enabling comparisons with the ordinary case.

The procedure in [12] is based on wavelets to extract the pulse at the beginning of a record and to determine its T_p. It also provides a score, a real number between 0 and 1, which is a function of the energy and amplitude of the pulse with respect to the recorded ground motion. In fact, the dataset considered herein is comprised of impulsive FN components from the NGA (Next Generation Attenuation project) database (http://peer.berkeley.edu/nga/) within 30 km from the source and with pulse score equal or larger than 0.85. This is the dataset also employed in [13], to which L'Aquila records analyzed in [2] plus the recording of the same event by the AQU station of the Mediterranean Network (MedNet, http://mednet.rm.ingv.it/) not yet available at the time of Ref. [2], were added.

For comparison, also records identified as non-pulse-like (i.e., ordinary) according to the discussed procedure, yet within 30 km from the source, were considered. Datasets, in terms of number of earthquake events and records, are summarized in Table I. Table II shows the distribution of pulse-

DOI: 10.1002/eqe

Table I. Pulse-like and ordinary datasets.

Mechanism	Earthquakes	Records	Earthquakes with pulse-like records	Pulse-like records
Strike–slip	22	133	12	34
Non-strike–slip	23	242	12	47
Total	45	375	24	81

Table II. Distribution of pulse-like records in T_p bins.

T_p	[0 s, 1 s[	[1 s, 2 s[	[2 s, 3 s[	[3 s, 4 s[	[4 s, 5 s[	[5 s, 6 s[	[6 s,12 s[
Number of records	22	20	8	11	10	5	5

like records in T_p bins. Moment magnitude ranges from 5.2 to 7.9 and the vast majority of records was from C and D NEHRP site classification.

The number of records from strike–slip events is 133, the records identified as pulses in the given dataset are 34. Records from other faulting mechanisms are in a single category because of their relative paucity summing up to 375, 81 of which are identified as containing pulses. Note that in the following no distinction of ground motion with different source parameters is considered, because results in [2] do not support it. This is also because, consistent with existing literature on the topic (e.g., [11]), the period[‡] (i.e., T_p) is expected to be the most important characteristic of this kind of ground motions.

In Figure 1(a) FN elastic spectra, normalized to PGA, are given for pulse-like records considered herein with T_P between 1 s and 2 s (*Average Pulse*) and for ordinary ground motions (*Average Non Pulse*). In Figure 1(b), C_R for R equal to 4 is also given for pulse-like and non-pulse-like records (*Pulse – FN* and *Non Pulse – FN*, respectively). For comparison, also C_R for the FP components of the pulse-like FN records (which are not necessarily pulse-like, even if indicated as *Pulse – FP*), are shown. The figures allow us to appreciate systematic differences summarized in Section 1, especially points (2) and (3), among the considered classes.[§] Moreover, it appears that FP records have a shape similar to FN in the low T/T_p range, yet with lower amplitudes. Same results hold for other R-values not shown.

3. FUNCTIONAL FORM AND REGRESSION STRATEGY

In FEMA 440 [14], the inelastic to elastic spectral response displacement coefficient, C_1 (referred to therein as the maximum displacement ratio), is given by the relationship in Equation (3), where α accounts for site subsoil conditions.

$$C_1 = 1 + (R-1)/\left(\alpha \cdot T^2\right) \tag{3}$$

As mentioned, among other researchers who have looked to near-source spectral amplification, the attention is focused herein on the work of Ruiz-Garcia [11], who, based on empirical evidence, proposed a functional form of C_R of the type in Equation (4) to account for a dominant frequency in ground motion.

$$C_R = 1 + \theta_1 \cdot \left(T_g/T\right)^2 \cdot (R-1) + \theta_2 \cdot \left(T_g/T\right) \cdot \exp\left\{\theta_3 \cdot \left[\ln\left(T/T_g - 0.08\right)^2\right]\right\} \tag{4}$$

[‡]In [11] this is concluded based on the *predominant period of ground motion*; it holds valid for T_p (to follow).
[§]The algorithm in [12] assigns a T_P also to ordinary records, rendering possible a representation as a function of T/T_P.

DOI: 10.1002/eqe

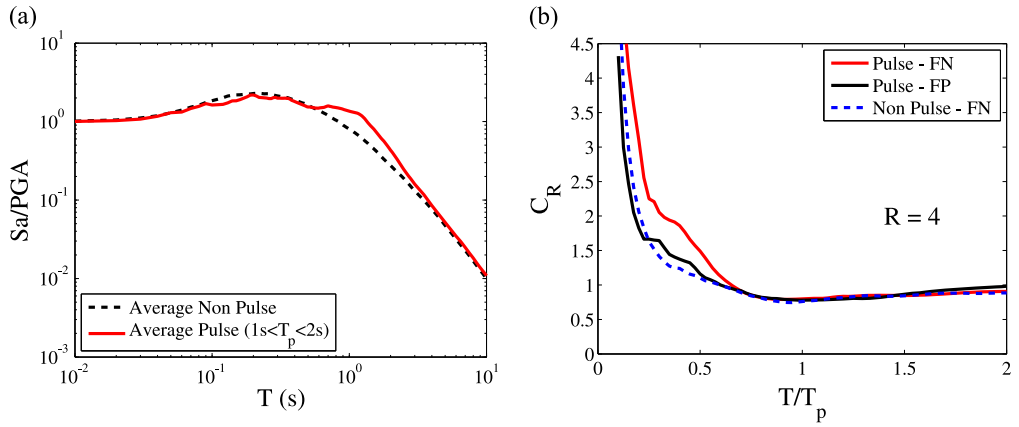

Figure 1. (a) Elastic 5% damped spectra for FN pulse-like with $1\,\mathrm{s} < T_\mathrm{P} < 2\,\mathrm{s}$ and ordinary records. (b) Empirical C_R for FN pulse-like records, for their FP components, and for ordinary records, at $R = 4$.

In this equation the first two terms are (intentionally) similar to Equation (3) and the third term is a function akin to a upside-down asymmetric bell (similar to a lognormal probability density function) centered at $T/T_\mathrm{g} \approx 1.0$, where T_g is the predominant period of ground motion, that is, the one corresponding to the peak of the 5% damped velocity spectrum. Although coefficient θ_1 appears in the same position as the α of Equation (3), it is not calibrated for local soil conditions. Because of the strong correlation existing between the two period measures, T_p and T_g (e.g., [11]), in the following T/T_p will be used in place of T/T_g.

It was noted in [11], and confirmed in the following, that Equation (4) is able to capture the shape of inelastic to elastic displacement ratio at $T/T_\mathrm{p} \approx 1$, while it is not able to capture the bump in the low T/T_p range. This calls for a modification of the prediction equation for C_R, which is investigated herein. Equation (5) consists of adding another term, like the last one in Equation (4), to reflect the C_R trend in the low T/T_p range (R dependency in the argument of the last term is explained in the following section). The resulting relationship has another bump (shifted and representing a peak rather than a valley). This equation has the same analytical form of that proposed in [8] for C_R in the case of soft soil sites. In fact, in that case, the SDOF response also is dominated by specific frequencies of ground motion, yet of a different nature.

$$C_\mathrm{R} = 1 + \theta_1 \cdot \left(T_\mathrm{p}/T\right)^2 \cdot (R-1) + \theta_2 \cdot \left(T_\mathrm{p}/T\right) \cdot exp\left\{\theta_3 \cdot \left[ln\left(T/T_\mathrm{p} - 0.08\right)\right]^2\right\} + \\ + \theta_4 \cdot \left(T_\mathrm{p}/T\right) \cdot exp\left\{\theta_5 \cdot \left[ln\left(T/T_\mathrm{p} + 0.5 + 0.02 \cdot R\right)\right]^2\right\} \tag{5}$$

To determine the coefficients of Equation (5) for each of the R-values considered, nonlinear-segmented regressions were applied for $0.1 \le T/T_\mathrm{p} \le 2$. The Levenberg–Marquardt algorithm [15], as implemented in MATLAB (Mathworks Inc., Natick, MA, USA) software, was employed. Moreover, the fitting was performed in two steps, such that the first three terms of Equation (5) were determined in the initial phase, then the residuals were computed and fitted via the fourth term; this was also to compare with Equation (4), and to determine efficiency of the considered functional form.

4. RESULTS AND DISCUSSION

The initial phase of the two-step procedure was to get coefficients for Equation (4), that is, the first three terms of Equation (5), Table III, for the bilinear SDOF systems herein investigated. This was carried out not considering data within the]0.35,0.775[T/T_p range. In fact, it fitted those segments of the forward-directivity data that seem to be captured by a relationship of the type in Equation (4) (Figure 2(a)).

DOI: 10.1002/eqe

Table III. Coefficient estimates for Equation (4).

	$R=2$	$R=3$	$R=4$	$R=5$	$R=6$	$R=7$	$R=8$
θ_1	0.0151	0.0209	0.0211	0.0198	0.0184	0.0170	0.0157
θ_2	−0.146	−0.230	−0.293	−0.343	−0.384	−0.417	−0.445
θ_3	−2.878	−2.360	−2.375	−2.437	−2.444	−2.441	−2.434

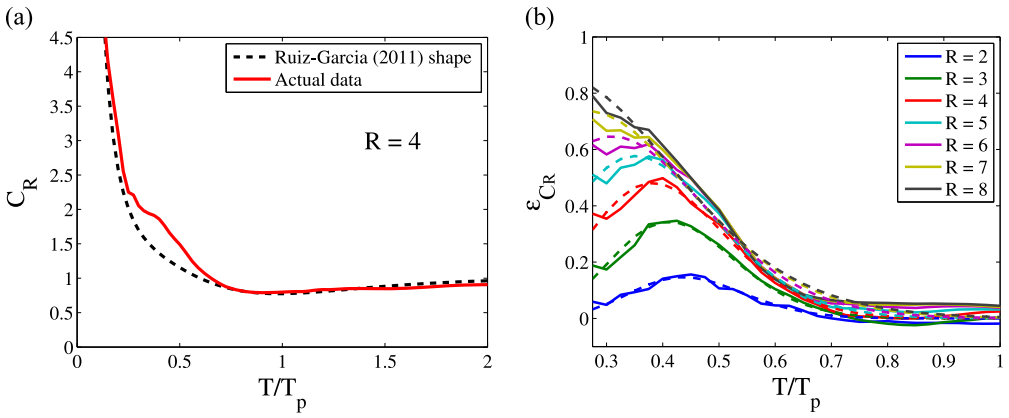

Figure 2. (a) Fitting of Equation (4) for pulse-like FN data ($R=4$) outside the]0.35,0.775[T/T_p range, and (b) fitting of Equation (6) for selected R-values.

The second step was to derive the residuals $(\varepsilon_{C_R})$of actual data with respect to Equation (4) and to fit them by the term in Equation (6), in which $\bar{C}_R$ is the data average, and $\hat{C}_R$ is the estimate from the model. This is similar to what was conducted in [16] to fit pulse-like ground motion elastic residuals to modify ordinary ground motion prediction equations. Table IV reports resulting coefficients.

$$\varepsilon_{C_R} = \bar{C}_R - \hat{C}_R \approx \theta_4 \cdot (T_p/T) \cdot \exp\left\{\theta_5 \cdot \left[\ln\left(T/T_p + 0.50 + 0.02 \cdot R\right)^2\right]\right\} \tag{6}$$

On the basis of Figure 2(b), it should be noted that the amplification observed in pulse-like records when compared with ordinary ground motions is around a T/T_p value whose location[¶] is a function of R. To capture this effect, the linear term $(0.50+0.02 \cdot R)$ appears in Equations (5) and (6).

Standard deviation (σ_{C_R}) was also fitted as a function of T/T_p and R. In fact, the functional form of the same type of Equation (5) was fitted on C_R plus one standard deviation data. Then, the relationship for σ_{C_R} was derived, Equation (7), whose coefficients are given in Table V. This may be considered the statistic of a lognormal random variable because it was found to be a more appropriate PDF, rather than Gaussian, for the observed data [17].

$$\sigma_{C_R} = 0.1 + s_1 \cdot (T_p/T)^2 \cdot (R-1) + s_2 \cdot (T_p/T) \cdot \exp\left\{\theta_5 \cdot \left[\ln\left(T/T_p + 0.50 + 0.02 \cdot R\right)\right]^2\right\} \tag{7}$$

In Figure 3(a) the composition of fitted coefficients of Tables III and IV to obtain the prediction relationship of the type in Equation (5), is given for all R-values investigated. As an example, actual data and fitted model are compared for R equal to 4 in Figure 3(b), in terms of average C_R and C_R plus one standard deviation. Goodness of fit holds for other R-values not shown.

[¶]For the sake of completeness it is to report that data, in the T/T_p range below 0.2, show another source of residual, for which Equation (5) does not attempt to account (in fact, it is not shown in Figure 2(b) which is plotted for larger T/T_P values). This unexplained residual has negligible effects on final fitting (i.e., Figure 3(b)); however, the interested reader may find details in [17].

DOI: 10.1002/eqe

Table IV. Coefficient estimates for Equation (6).

	$R=2$	$R=3$	$R=4$	$R=5$	$R=6$	$R=7$	$R=8$
θ_4	0.066	0.146	0.193	0.217	0.224	0.232	0.242
θ_5	−47.931	−40.966	−32.697	−27.173	−20.973	−17.211	−15.177

Table V. Standard deviation coefficients for Equation (7).

	$R=2$	$R=3$	$R=4$	$R=5$	$R=6$	$R=7$	$R=8$
s_1	0.0170	0.0278	0.0306	0.0294	0.0262	0.0232	0.0208
s_2	0.0635	0.0837	0.0657	0.0516	0.0516	0.0485	0.0400

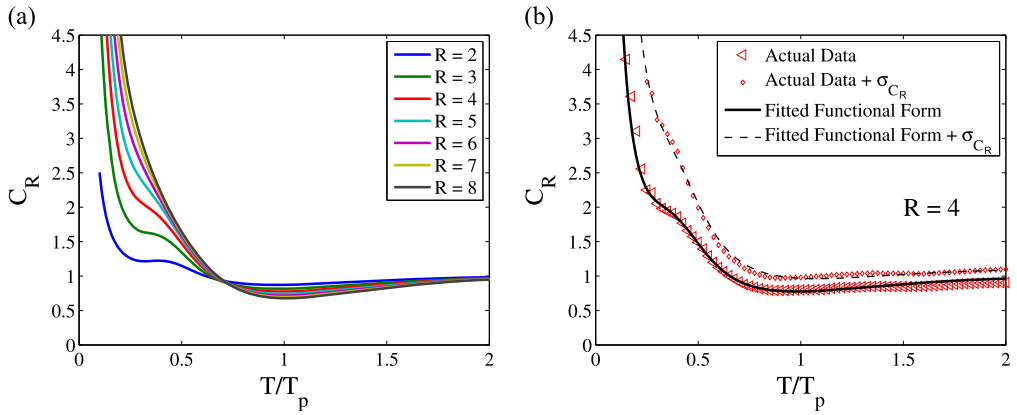

Figure 3. (a) Double-bump fitted C_R trends and (b) comparison with empirical data for $R=4$.

5. CONCLUSIONS

In the presented study the functional form for prediction of near-source pulse-like inelastic displacement ratio was investigated. This is required for structural assessment procedures in near-source conditions, and complements current efforts to model effects of forward directivity on elastic seismic structural demand, that is, seismic hazard.

It was found that an additional term is necessary with respect to those used to fit trends from ordinary ground motion as a function of T/T_p. An asymmetric-bell term, centered at different points depending on R, was suitable to fit C_R in the low T/T_p range. This resulted in two opposite bumps in two different spectral regions, and builds up consistently with recent literature on the same topic and on what is observed for soft soil site records, which are also characterized by a predominant period.

Coefficients for this relationship were determined in a two-step nonlinear regression, for a range of strength reduction factors, of a relatively large set of fault normal pulse-like records. Finally, standard deviation of residual data was also fitted by an analytical equation as a function of the T/T_p ratio. These results may be of some help in investigations concerning design procedures specific for near-source conditions, given that the pulse period is available from design scenarios based on near-source probabilistic seismic hazard analysis.

ACKNOWLEDGEMENTS

The study presented in this paper was developed within the activities of *Rete dei Laboratori Universitari di Ingegneria Sismica* (ReLUIS) for the research program funded by the *Dipartimento della Protezione Civile* (2010–2013).

DOI: 10.1002/eqe

REFERENCES

1. Somerville PG, Smith NF, Graves RW, Abrahamson NA. Modification of empirical strong motion attenuation relations to include the amplitude and duration effect of rupture directivity. *Seismological Research Letters* 1997; **68**(1): 199–222.
2. Chioccarelli E, Iervolino I. Near-source seismic demand and pulse-like records: a discussion for L'Aquila earthquake. *Earthquake Engineering and Structural Dynamics* 2010; **39**(9):1039–1062.
3. Tothong P, Cornell CA, Baker JW. Explicit directivity-pulse inclusion in probabilistic seismic hazard analysis. *Earthquake Spectra* 2007; **23**(4):867–891.
4. Shahi S, Baker JW. An empirically calibrated framework for including the effects of near-fault directivity in probabilistic seismic hazard analysis. *Bulletin of the Seismological Society of America* 2011; **101**(2):742–755.
5. Chioccarelli E, Iervolino I. Near-source seismic hazard and design scenarios, 2011. (in review)
6. Ruiz-Garcìa J, Miranda E. Inelastic displacement ratios for evaluation of existing structures. *Earthquake Engineering and Structural Dynamics* 2003; **32**(8):1237–125.
7. Fajfar P. Capacity spectrum method based on inelastic demand spectra. *Earthquake Engineering and Structural Dynamics* 1999; **28**(9):979–993.
8. Ruiz-Garcìa J, Miranda E. Inelastic displacement ratios for evaluation of structures built on soft soil sites. *Earthquake Engineering and Structural Dynamics* 2006; **35**(6):679–694.
9. Baez JI, Miranda E. Amplification factors to estimate inelastic displacement demands for the design of structures in the near field. *Proc. of the Twelfth World Conference on Earthquake Engineering*, Auckland, NZ, 2000; paper no. 1561.
10. Akkar SD, Yazgan U, Gulkan P. Deformation limits for simple non-degrading systems subjected to near-fault ground motions. *Proc. of the Thirteen World Conference on Earthquake Engineering*, Vancouver, CAN, 2004; paper no. 2276.
11. Ruiz-Garcìa J. Inelastic displacement ratios for seismic assessment of structures subjected to forward-directivity near-fault ground motions. *Journal of Earthquake Engineering* 2011; **15**(3):449–468.
12. Baker JW. Quantitative classification of near-fault ground motions using wavelet analysis. *Bulletin of the Seismological Society of America* 2007; **97**(5):1486–1501.
13. Iervolino I, Cornell CA. Probability of occurrence of velocity pulses in near-source ground motions. *Bulletin of the Seismological Society of America* 2008; **98**(5):2262–2277.
14. Federal Emergency Management Agency. Improvement of nonlinear static seismic analysis procedures. Report FEMA 440. Washington DC, US, 2005.
15. Bates DM, Watts DG. *Nonlinear regression analysis and its applications*. Wiley: New York, 1988.
16. Baker JW. Identification of near-fault velocity and prediction of resulting response spectra. *Proceeding of Geotechnical Earthquake Engn. Struct. Dyn. IV*, Sacramento, CA, 2008.
17. Baltzopoulos G. Effect of near-source directivity on inelastic spectral amplification. Earthquake Resistant Structural Design M.Sc. Thesis, Aristotle University of Thessaloniki, Greece, Advisor: I. Iervolino, 2011.

DOI: 10.1002/eqe